Kinetic Target-Guided Synthesis of Small-Molecule G-Quadruplex Stabilizers

Alice Pomeislová[+],[a, b] Lukáš Vrzal[+],[a, c] Jaroslav Kozák,[a] Juraj Dobiaš,[a] Martin Hubálek,[a] Hana Dvořáková,[c] Paul E. Reyes-Gutiérrez,[a] Filip Teplý,[a] and Václav Veverka*[a, d]

The formation of a G-quadruplex motif in the promoter region of the *c-MYC* protooncogene prevents its expression. Accordingly, G-quadruplex stabilization by a suitable ligand may be a viable approach for anticancer therapy. In our study, we used the 4-(4-methylpiperazin-1-yl)aniline molecule, previously identified as a fragment library screen hit, as a template for the SAR-guided design of a new small library of clickable fragments and subjected them to click reactions, including kinetic target-guided synthesis in the presence of a G-quadruplex forming oligonucleotide Pu24. We tested the clickable fragments and products of click reactions for their G-quadruplex stabilizing activity and determined their mode of binding to the *c-MYC* G-quadruplex by NMR spectroscopy. The enhanced stabilizing potency of click products in biology assays (FRET, Polymerase extension assay) matched the increased yields of in situ click reactions. In conclusion, we identified the newly synthesized click products of bis-amino derivatives of 4-(4-methylpiperazin-1-yl)aniline as potent stabilizers of *c-MYC* G-quadruplex, and their further evolution may lead to the development of an efficient tool for cancer treatment.

1. Introduction

Poly-guanine tracts in nucleic acids form non-canonical structures known as G-quadruplexes (G4s), which were recognized as an attractive class of targets for therapeutic intervention in cancer,[1–3] particularly for their role in regulating the expression of key oncogenes.[4] It was found that stabilization of G4 near the *c-MYC* gene promoter using a small molecule can reduce the levels of the *c-MYC* oncoprotein in the nucleus.[5] Increased *c-MYC* oncoprotein expression is typical of many cancers and often associated with poor prognosis (aggressive tumors, poor clinical outcome and increased metastasis, recurrence and mortality rates).[6–9] Therefore, G4 stabilization to reduce *c-MYC* expression is one of the potential anticancer strategies.[4,9]

The G4 motif, a key regulatory element of the human *c-MYC* gene,[10] is located downstream of the promoter region of the *c-MYC* gene in the nuclease hypersensitive element III_1 (NHE III_1) that controls over 80% of the *c-MYC* transcriptional activity.[5,11] The NHE III_1 comprises the core 27-nucleotide sequence of the wild-type *c-MYC* (Pu27) that contains six guanine tracts and can thus form multiple G4s.[5,12–15] Apart from that, other biologically relevant sequences have been described, e.g., the 'propeller type' parallel-stranded G4 sequence containing the four central guanine tracts of Pu27, or the 24-nucleotide five-guanine-tract sequence (Pu24) forming a parallel-stranded foldback G4.[13]

Generally, the *c-MYC* ligands are planar aromatic molecules that interact with the G4 scaffold via external π-π stacking. In addition, electrostatic interactions between positively charged ligands and negatively charged G4-DNA scaffolds contribute to G4 stabilization.[16] The known *c-MYC* binders include e.g., the cationic porphyrin TMPyP4,[5] the synthetic fluorescent dye Hoechst 33258,[17–18] quindoline[19–20] and berberine[21] derivatives, carbazoles,[22] perylene derivatives,[23] the fluoroquinolone derivative quarfloxin,[24–25] and the 1,4-dihydroxyanthracene-9,10-dione derivative MYRA-A.[26] More recently, various 4-anilinoquinazoline derivatives[27] as well as the crescent-shaped thiazole peptide TH3[28] were found to down-regulate transcription and expression of the *c-MYC* gene in HeLa cells. Other newly reported *c-MYC* ligands comprised functionalized imidazo[2,1-*i*]purine derivatives[29] and fluorescent binaphthyl amines.[30]

The rational design of novel potent and selective G4 ligands is inherently difficult due to the dynamic nature of typical G4 structures.[13] Recently, kinetic target-guided synthesis (KTGS) proved successful in the development of novel inhibitors of several enzymes with improved selectivity.[31–36] In KTGS, the target molecule is exploited to irreversibly assemble its own

[a] *A. Pomeislová,[+] Dr. L. Vrzal,[+] Dr. J. Kozák, Dr. J. Dobiaš, Dr. M. Hubálek, Dr. P. E. Reyes-Gutiérrez, Dr. F. Teplý, Dr. V. Veverka*
Institute of Organic Chemistry and Biochemistry
The Czech Academy of Sciences
Flemingovo nam. 2
Prague (Czech Republic)
E-mail: vaclav.veverka@uochb.cas.cz
[b] *A. Pomeislová,[+]*
Department of Organic Chemistry
Charles University
Prague (Czech Republic)
[c] *Dr. L. Vrzal[+] Dr. H. Dvořáková*
NMR laboratory
University of Chemistry and Technology
Prague (Czech Republic)
[d] *Dr. V. Veverka*
Department of Cell Biology
Charles University
Prague (Czech Republic)
[+] *These authors contributed equally to this work*

Supporting information for this article is available on the WWW under https://doi.org/10.1002/open.202000261

inhibitor (ligand) in situ by joining two suitable fragments with complementary reactive groups via a 'click reaction'. This term typically refers to a 1,3-dipolar cycloaddition between azides and terminal alkynes that leads to triazole formation, although there are several alternative reactions (as reviewed in ref.[37]). Specific interactions between fragments and the biological target bring the two molecules into close proximity with a suitable orientation, which decreases the negative $\triangle S^{\neq}$ values of 1,3-dipolar cycloaddition, thereby overcoming the otherwise low reaction rate under non-catalyzed conditions. During in situ click experiments, the target molecule controls the assembly of the best alkyne and azide within a pool of available fragments present in the reaction mixture. By directing the choice of the best binding partner, the active site of a biological target promotes the synthesis of the most efficient ligand/inhibitor.[31–36,38–40] KTGS employing in situ click chemistry allows to build novel and unique ligands by combining suitable fragments and to improve previously established ligands towards fine-tuning their selectivity and bioavailability.[41] To date, KTGS has been only used to stabilize telomeric G4.[38–39]

Here, we present the in situ development of *c-MYC* G4 stabilizers by KTGS using a 4-(4-methylpiperazin-1-yl)aniline molecule that was active in the previous library screen targeting *c-MYC* G4.[42] We successfully modified this scaffold for click chemistry and prepared a series of compounds through both in situ and conventional chemical synthesis. The clickable fragments and the synthesized click products were tested for their G4 stabilizing activity, and their mode of binding to *c-MYC* G4 was characterized using NMR spectroscopy. The combination of biochemical assays, in situ click experiments, and NMR data provided a basis for the characterization of structure-activity relationships that led to the successful development of *c-MYC* G4 stabilizers.

2. Results and Discussion

2.1. Choice of Fragment Template

Initially, we tested the 11 fragments (Figure 1), which were reported by Nasiri et al[42] as *c-MYC* ligands, in *in vitro* assays to evaluate their *c-MYC* G4-stabilizing potential. In particular, we employed a standard polymerase extension assay (PEA) using a template strand containing the Pu27 sequence and tested thermal stabilization of G4-forming Pu25 oligonucleotide detected by Förster resonance energy transfer (FRET). All compounds from this set produced a stop band in PEA at 500 μM, and compound **7** was the strongest G4 stabilizer (ESI, Section 3.1, Figure S3.1 and S3.2). In addition, compound **7** induced a significant thermal stabilization effect on the labeled Pu25 oligonucleotide in FRET, with a melting temperature increase of $10.4 \pm 0.6\,^{\circ}C$ at 100 μM, indicating that this compound has a significantly higher binding affinity to *c-MYC* G4 than other compounds in the respective set (data not shown).

Additionally, a significant fraction of compound **7** is incorporated into the fluorescent dye Hoechst 333258 that was previously reported as a *c-MYC* ligand.[43–44] Therefore, we decided to use the structure of **7** as a template to build a focused fragment library through synthetic elaboration.

2.2. Focused Fragment Library

In order to design new molecules with enhanced *c-MYC* affinity, we aimed to construct a small focused fragment library derived from compound **7** that would be amenable for KTGS. Before functionalizing compound **7** for click chemistry, it was necessary to ascertain the role of various chemical moieties of this parent compound **7** in *c-MYC* stabilization. For this purpose, a set of commercially available derivatives of compound **7** that contained modifications at the piperazine and/or at the aniline moiety was provided (Figure 2, **12**–**23**). All the compounds **12**–**23** were tested in FRET melting assay and in PEA at 100 μM for their *c-MYC* binding ability and compared to the parent compound **7** (for PEA gel images, see ESI, Section 3.2, Fig-

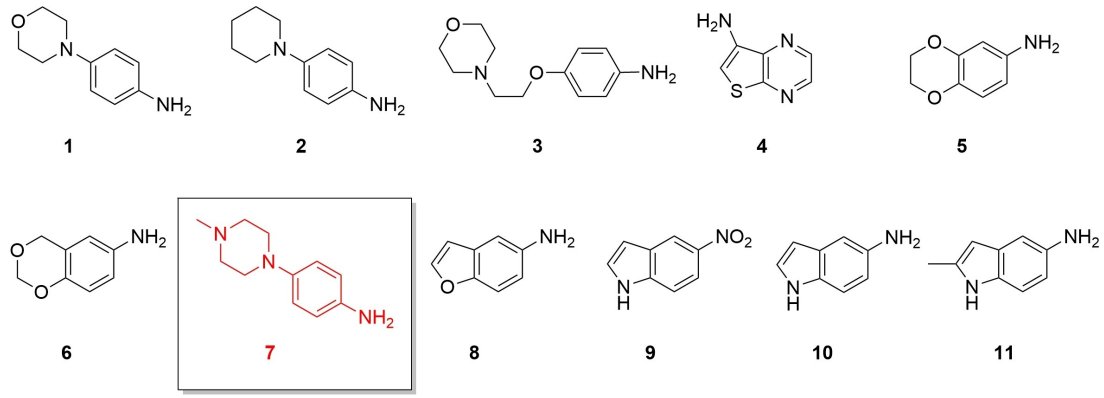

Figure 1. The 11 published compounds (**1**-**11**) which were found as *c-MYC* ligands in a previously performed fragment library screen.[42] The FRET and PEA assays suggested fragment **7** as the best ligand and it was therefore selected for further elaboration.

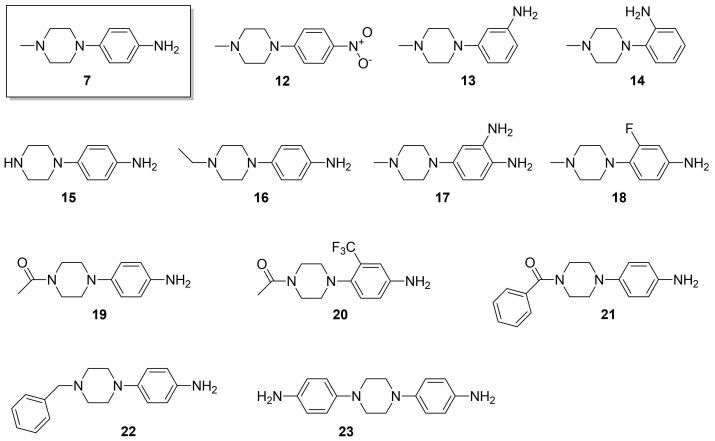

Figure 2. A set of 4-(4-methylpiperazin-1-yl)aniline derivatives containing various chemical moieties. Compounds **12**–**23** were obtained from commercial sources.

ure S3.3 and S3.4). The only molecule that exhibited significantly increased FRET activity and retention of PEA activity compared to compound **7** was the bis-amino derivative **17** containing an additional amino moiety in position 2 of the aromatic ring. With ΔT_m increase exceeding 35 °C, compound **17** exhibited more than 3-fold ΔT_m increase in FRET relative to the parent molecule **7**. Furthermore, the reduced activity of the nitro analogue **12** and inactivity of the compounds **13** and **14** isomeric to **7** suggested necessity of the amino group at the *para*-position of the aromatic ring for interaction of the ligand with *c-MYC*. Therefore, this amino moiety cannot be used for further derivatization. Finally, inactivity of compound **15** with an unsubstituted N^4-piperazine position and partial restoration of PEA activity for compound **16** underlines the need of an aliphatic substituent at this piperazine nitrogen.

Based on these findings, we constructed a fragment library (Figure 3A and 3B) that consisted of two different families of *N*-alkyne compounds: a mono-amino series directly derived from **7** (Figure 3A) and a bis-amino series containing an additional amino functional group at position 2 of the aromatic ring (Figure 3B). Both series included 'clickable' compounds alkynylated at the N^4-piperazine position and the resulting click products. The design of both series was guided by a SAR study performed simultaneously with compound synthesis.

The mono-amino series was synthesized by *N*-alkylation of the piperazine moiety of 4-(piperazin-1-yl)aniline (compound **15**) with three different alkynyl halides of various chain lengths to investigate influence of molecule flexibility on interaction with *c-MYC*. Thus, we prepared a homologous series of three alkynes with 1, 2 or 3 methylene units in the alkynyl chain, that is, **24**,[45] **25**, and **26** (Figure 3A), respectively. Compounds **24**–**26** were directly coupled to four selected azides **52**–**55** (Figure 3C) in a Cu^I-catalyzed 1,3-dipolar cycloaddition (CuAAC), referred to as 'click reaction', upon 1,4-triazole formation (products **27**–**38**, Figure 3A).[38] The choice of azides **52**–**53** and **55** was directly inspired by the study performed by Di Antonio et al[38] and azide **54** was included as a tertiary-amine analogue to compound **53**. The click product **40**, a nitro analog of **38**, was obtained from the nitro-alkyne **39** and served as a negative control to assess whether the amino group is essential for electrostatic interactions between the fragments and the *c-MYC* G4. Similarly, compound **12** served as a negative control for comparison with **7**.

The bis-amino series (Figure 3B) was prepared by nucleophilic aromatic substitution of 5-chloro-2-nitroaniline with piperazine, resulting in compound **41**[46] with a nitroaniline moiety, which was then reduced by Pd/C under hydrogen atmosphere to **42**.[46] Compound **42**, which contains an *o*-phenylendiamine moiety, was *N*-alkylated with three alkynyl halides of different linker length to form the homologous series of compounds **43**–**45** (Figure 3B) carrying 1–3 methylene units in the alkynyl chain. Within this bis-amino series, we decided to prepare only click products derived from alkyne **45** with 3 methylene units because the previously performed SAR study regarding the mono-amino series (Table 2 for PEA results, and Table 3 for in situ click results) showed that the Pu27-stabilizing activity of click products **35** and **38** positively correlated with the length of the alkynyl linker: the *N*-alkynyl chain with three methylene units showed the best Pu27 stabilizing activity. Furthermore, azides **54** and **55** provided the most active mono-

Table 1. FRET and PEA results at 100 μM for commercial compound **7** derivatives **12**–**23** in comparison to the parent molecule **7**.

Cpd. No	PEA at 100 μM	ΔTm/°C FRET at 100 μM
7	1.0	10.4 ± 0.6
12	0.2	3.7 ± 0.5
13	0.2	0.0
14	–	−0.3
15	0.2	1.6
16	0.6	1.7
17	1.1	> 35
18	0.2	1.1
19	0.3	1.8
20	0.1	0.9
21	0.2	1.2
22	0.2	1.1
23	0.2	1.1

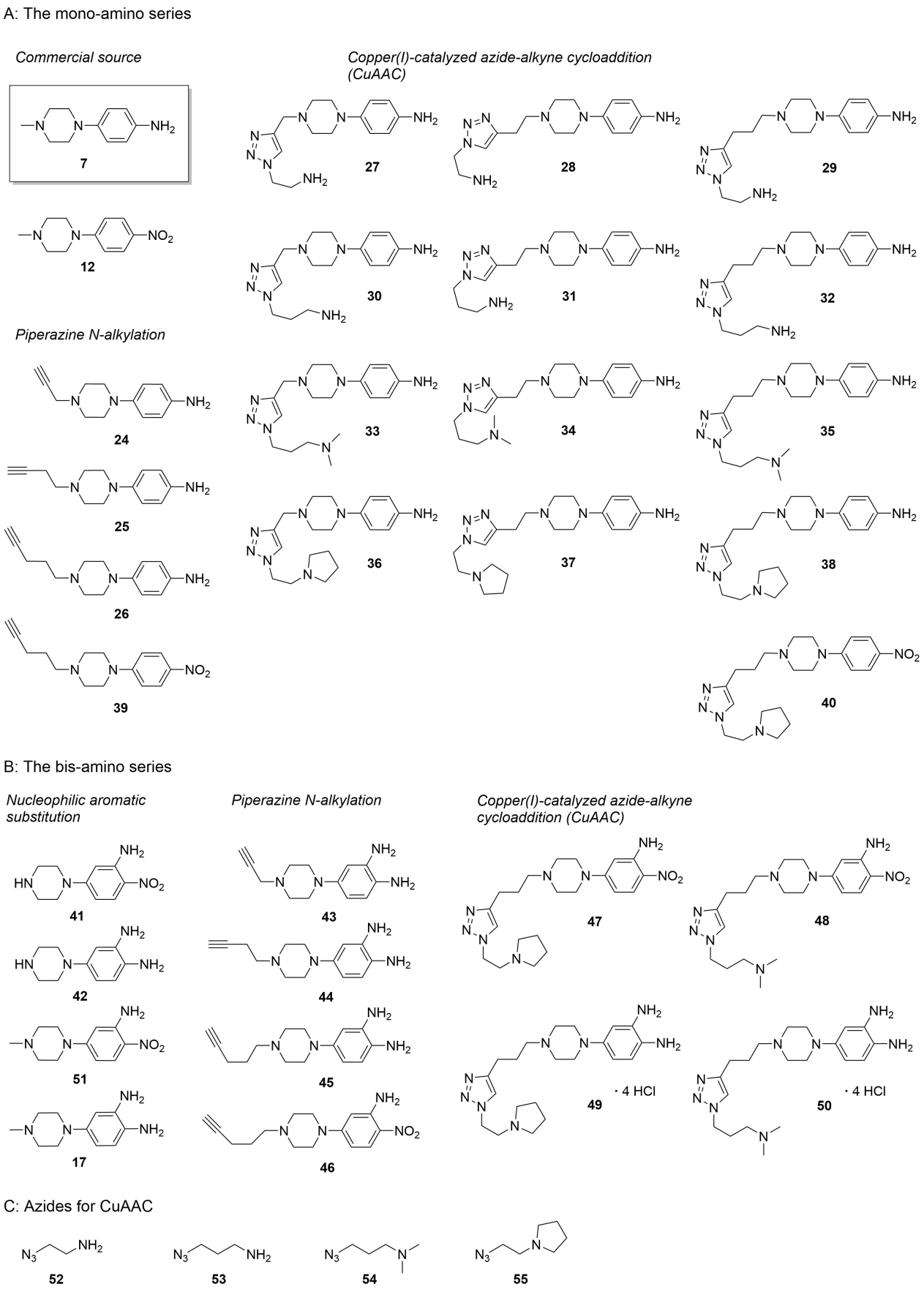

Figure 3. 4-(piperazin-1-yl)aniline-derived fragment library constructed in the present study. (A) Mono-amino series. (B) Bis-amino series. (C) Azides used for CuAAC. Compounds from both series (A and B) are sorted by type of reaction whereby they were prepared.

Table 2. SAR data summary showing both the FRET and PEA results at 100 μM. The PEA values (ESI, Section 3.3, Supplementary Figure S3.5–S3.9) are determined as a quotient of stop band density of the respective compound divided by the stop band density of the parent compound **7**.

Cpd. No	Structure	PEA at 100 μM	ΔTm/°C FRET at 100 μM
7	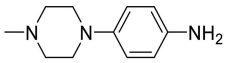	1.0	10.4 ± 0.6
12	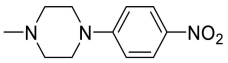	0.5	3.7 ± 0.5
24	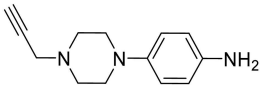	0.1	3.3 ± 0.4
25	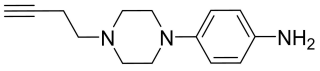	0.1	2.4 ± 0.9
26	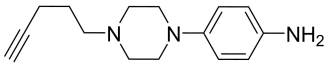	0.5	2.4 ± 0.4
27	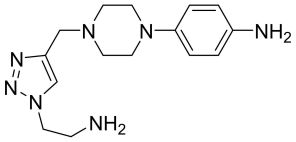	0.4	−2.3 ± 0.7
28	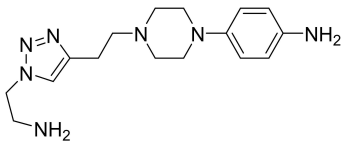	0.5	−1.9 ± 0.3
29	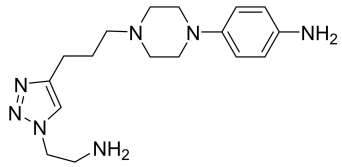	0.5	−2.7 ± 0.2
30	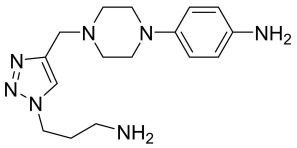	0.6	−1.4 ± 0.3
31	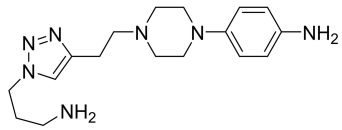	0.5	−2.5 ± 0.4
32	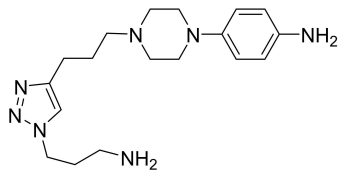	0.7	−2.3 ± 0.3
33	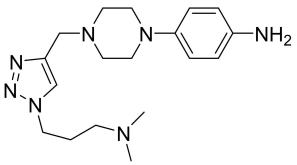	0.7	3.6 ± 0.5
34	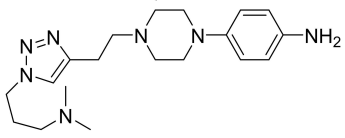	0.9	3.6 ± 0.8

Table 2. continued

Cpd. No	Structure	PEA at 100 μM	ΔTm/°C FRET at 100 μM
35	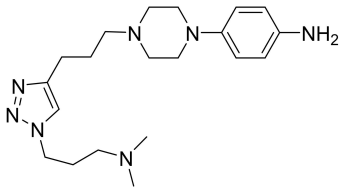	0.8	4.2 ± 0.8
36	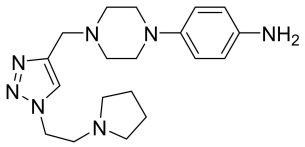	0.5	3.0 ± 0.8
37	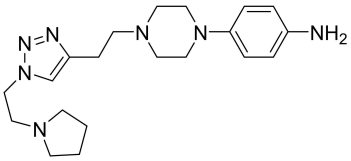	0.6	3.9 ± 0.4
38	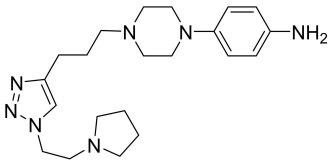	1.2	7.6 ± 0.4
40	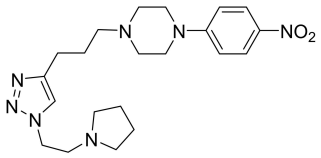	0.1	3.9 ± 0.1
41	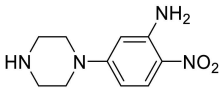	0.3	4.1 ± 1.1
42	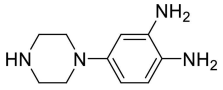	1.6	> 35
43	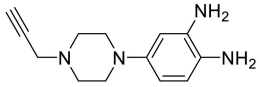	0.5	13.0 ± 0.9
44	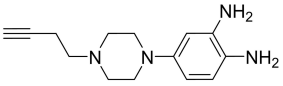	0.5	15.9 ± 1.0
45	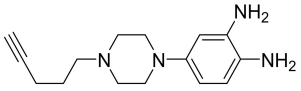	1.6	29.5 ± 0.3
46	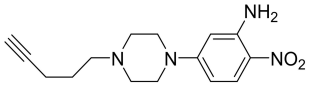	0.1	5.6 ± 0.4
47	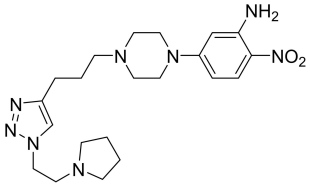	0.5	3.5 ± 0.4

Table 2. continued

Cpd. No	Structure	PEA at 100 μM	ΔTm/°C FRET at 100 μM
48	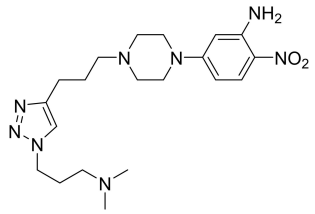	0.7	5.1 ± 0.7
49	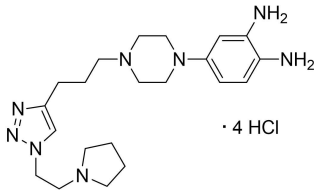 · 4 HCl	4.5	33.9 ± 0.2
50	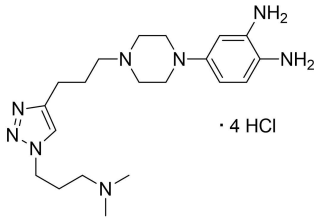 · 4 HCl	4.5	> 35
51	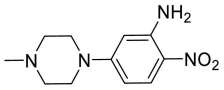	0.1	1.0 ± 1.0
17	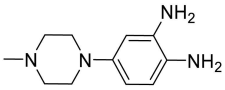	1.6	> 35

amino click products. However, the analogous direct click reaction of the bis-amino alkyne derivative **45** with azides **54** and **55** was not performed due to the low stability of the *o*-phenylendiamine moiety. Instead, *o*-nitroaniline compound **41** was alkylated with 5-iodopent-1-yne to form **46**. In a CuAAC[38] with azides **54** and **55**, alkyne **46** formed triazoles **47** and **48**, respectively. The resulting *o*-nitroaniline click products **47** and **48** were subsequently reduced by Pd/C under hydrogen atmosphere to their diamino counterparts, **49** and **50**, and immediately converted into hydrochloride salts to stabilize them. Lastly, compounds **51** and **17** (Figure 3B), bis-amino analogs of **7**, were prepared as described for compounds **41** and **42**, respectively: in a nucleophilic aromatic substitution with 1-methylpiperazine, 5-chloro-2-nitroaniline formed compound **51**; compound **17** was then prepared from **51** by reduction of the nitro group by Pd/C under hydrogen atmosphere.

In conclusion, FRET and PEA evaluation of various 4-(piperazin-1-yl)aniline derivatives showed that the amino group at the *para*-position of the aromatic ring was found necessary for interaction of the ligand with *c-MYC*. Also, an additional amino moiety in position 2 of the aromatic ring further increased the *c-MYC* stabilizing potency. Therefore, we constructed a fragment library that contained the mono-amino series directly inspired by the parent **7** molecule and the bis-amino series with an additional NH_2- group. Both series included the clickable fragments alkynylated on the piperazine nitrogen as well as the respective click products resulting from CuAAC with selected cationic azides.

2.3. Structure-Activity Relationships

Here, we investigated how different chemical moieties, present in compound **7** derivatives, and their respective positions contribute to *c-MYC* G4 stabilization. For this purpose, a starting ligand concentration of 100 μM was used in both the FRET and PEA biochemical assays; the results are compared to the parent compound **7** and summarized in Table 2 (for PEA gel images, see ESI, Section 3.3, Figure S3.5 to S3.9.

Amino groups are a common feature of well-established G4 ligands because they bind to phosphate groups of the G4 backbone via electrostatic interactions mediated by bridging water molecules.[47] As expected, the fragments containing amino groups **7** and **17** exhibited higher stabilization activity at 100 μM in both FRET and PEA than their nitro analogs **12** and **51**, respectively (Table 2), suggesting that a free amino group in *para*-position of the aromatic ring is required for the interaction between the ligand and the *c-MYC* G4. Additionally, a higher number of amino groups also showed enhanced *c-MYC* affinity (Table 2, e.g., **17** versus **7**). These results confirm the original findings obtained during FRET and PEA evaluation of commercial derivatives of compound **7** (Table 1).

Apart from that, we found that the piperazine moiety of 4-(piperazin-1-yl)aniline can be *N*-alkylated at the N^4 position by different-length alkynyl groups (with one to three methylene units) without affecting its ability to bind to G4. This was observed in scaffolds derived from the compound **17** carrying two amino groups at the aromatic ring (**43**–**45**), whereas the activity was abolished in mono-amino derivatives (**24**–**26**). Interestingly, we observed considerable restoration of the G4 stabilizing activity for the click products **34**–**35** (in PEA) and **38** (in both PEA and FRET), all of which were prepared from the *N*-alkynylated mono-amino derivatives (Table 2). In general, click products **33**–**38**, derived from compounds **54** and **55**, exhibited partially restored FRET and PEA activity when compared to the parent compound **7**, although the extent of activity restoration varied widely. Nevertheless, all these click products showed overall better activity than click products **27**–**32**, derived from **52** and **53**, which exhibited a small decrease in Pu25 melting temperature in FRET at 100 μM, indicating their inactivity. Moreover, the click product **38** derived from compound **26** with three methylene units in the alkynyl linker was more active in both FRET and PEA than its shorter-linker analogs, compounds **36** and **37**. A similar trend was also observed in FRET for the click product **35** and its analogs **33** and **34**, although the difference in activity was rather small. It is obvious that increased flexibility of the central part of the molecule facilitates interaction of certain ligand moieties with *c-MYC*. Accordingly, previously performed studies[48–51] also reported the impact of the linker length or side-chain length and thus molecule flexibility on interaction with various G4 s. Taken together, these

Table 3. The relative formation yields of compounds **27**–**38** given by reaction ratios. X-1, Y-1, and Z-1-the combination reactions of three alkynes with the corresponding azides; A, B and C-in situ click reactions with and without Pu24 and a control reaction, respectively. The ratio was calculated by comparing the area of specific m/z value from the extracted ion chromatography in LC-MS experiment.

Compound		CH_2 units	Experiment X-1 A/B	Experiment X-1 A/C	Experiment Y-1 A/B	Experiment Y-1 A/C	Experiment Z-1 A/B	Experiment Z-1 A/C
27	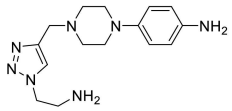	1	1.8	1.3	–	–	–	–
28	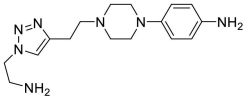	2	1.7	1.3	–	–	–	–
29	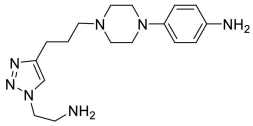	3	4.4	3.0	–	–	–	–
30	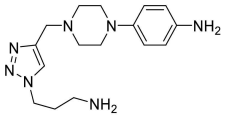	1	–	–	1.4	1.2	–	–
31	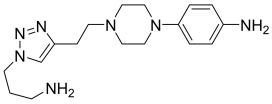	2	–	–	1.5	1.2	–	–
32	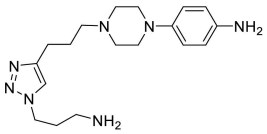	3	–	–	2.5	1.9	–	–
33	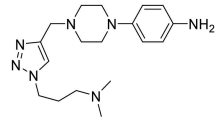	1	7.1	4.7	–	–	6.6	5.1
34	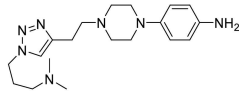	2	5.2	3.1	–	–	7.4	4.4
35	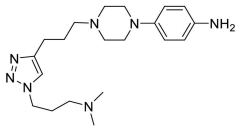	3	22.7	10.8	–	–	55.0	42.7
36	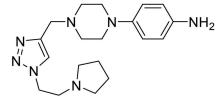	1	–	–	4.8	3.8	5.4	4.5
37	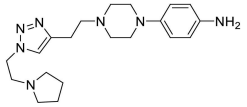	2	–	–	3.4	2.5	3.7	2.6
38	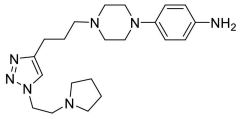	3	–	–	9.8	5.5	16.9	10.5

results show that a simple N^4-alkynylation of the piperazine moiety at the 4-(piperazin-1-yl)aniline template can destroy the binding activity of the resulting mono-amino fragment, but an additional click reaction of the inactive molecule with a suitable azide can lead to a click product with partly restored activity.

Generally, the bis-amino series exhibited higher affinity towards *c-MYC* than the mono-amino series. The FRET activity of piperazine-alkylated bis-amino compounds **43**–**45** was lower than that of the bis-amino standard **17**, albeit similar to or better than the activity of the mono-amino template **7**. Both bis-amino click products **49** and **50** exhibited a significant increase in activity in FRET experiments at 100 μM, which was comparable to that of **45** and **17** and even 3-fold higher than the activity of **7** (Table 1). Moreover, based on PEA measure-

ments, **49** and **50** appeared to be strongest ligands prepared in this study with 4.5-fold activity increase compared to compound **7** and significantly higher activity than **45** and **17**. The inactivity of the parent nitroaniline compounds **47** and **48** underlines the importance of the aromatic 1,2-diamino moiety in **49** and **50** for Pu27 stabilization potency.

Interestingly, the alkynylated derivatives of both series as well as most mono-amino click products exhibited decreased activity when compared to the respective parent molecule **7** or **17**. We hypothesize that alkynylated derivatives and click products interact with the G4 structure via both the 4-(piperazin-1-yl)-aniline motif and the alkynyl chain or triazole residue, respectively. If the linker connecting the piperazinyl moiety with the triple bond or triazole ring is short, the molecule is rigid and interacts with G4 via both moieties inefficiently. This leads to activity decrease of such fragment. On the other hand, three methylene units in the linker provide the molecule with increased flexibility that facilitates effective binding of the molecule to the G4 structure via both moieties. This way we could explain activity restoration in the case of the mono-amino click product **38** and the bis-amino alkyne **45**, and PEA activity increase in the case of the bis-amino click products **49** and **50**.

As compounds **42**–**45**, **49**–**50**, and **17** from the bis-amino series exhibited sufficiently increased *c-MYC* stabilization potential at 100 μM, they were also evaluated by comparative FRET assay at 50 μM together with their *o*-nitroanaline analogues **41**, **46**–**48**, and **51** for their G4-specificity over duplex DNA; the parent compound **7** and its nitro-analogue **12** were included for comparison. Therefore, apart from using F-myc25T, all these compounds were tested in control FRET experiments with a dual-labelled FdsT oligonucleotide containing a 26-mer 'Q sequence' (ds26) that forms a double-stranded hairpin.[52] The FRET results for F-myc25T and FdsT at 50 μM are displayed in Figure 4 (FRET data available in ESI, Section 3.5, Table S3.1). The data regarding *c-MYC* stabilization showed significantly increased ΔT_m values of the amino-, resp. bis-amino derivatives in comparison with their nitro-, resp. *o*-nitroaniline analogs. In addition, the FRET activity of the homologous series of bis-amino alkynes **43**–**45** at 50 μM increased with the number of methylene units in the alkynyl linker, which is in line with the FRET measurements at 100 μM (Table 2). The control FRET experiments with FdsT showed in most cases zero stabilization potential at 50 μM. Although a slight ΔT_m increase was observed for compound **42**, the value was negligible when compared to ΔT_m increase induced for *c-MYC* (F-myc25T) stabilization. Therefore, we can conclude that our ligands, especially the bis-amino compounds **17**, **42**, **45**, **49**, and **50**, selectively interact with the *c-MYC* G4 motif.

The compounds **17**, **42**, **45**, **49**, and **50** were tested in a competitive FRET assay at 25 μM and 10 μM concentration. For each ligand concentration, two parallel FRET experiments were performed: one with F-myc25T (0.2 μM), and the second with the mixture of F-myc25T (0.2 μM) and 10-fold excess of non-labelled oligonucleotide ds26 (2.0 μM). The results are summarized in Figure 5 (FRET data available in ESI, section 3.5, Table S3.2). In spite of an apparent ΔT_m decrease in competitive

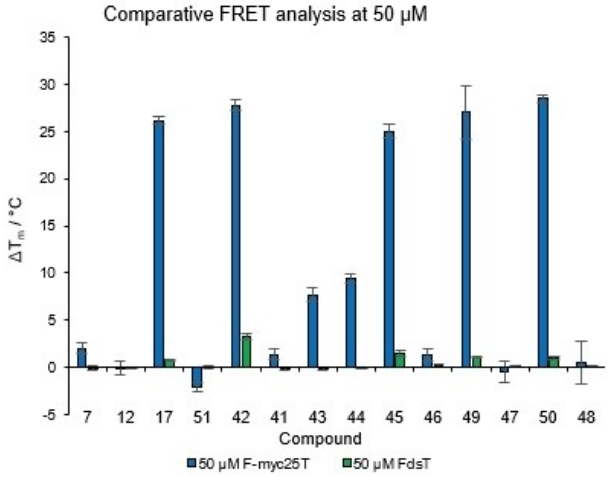

Figure 4. Comparative FRET analysis at 50 μM using F-myc25T and FdsT (control), performed with the bis-amino series in compaison to compounds **7** and **12** of the mono-amino series.

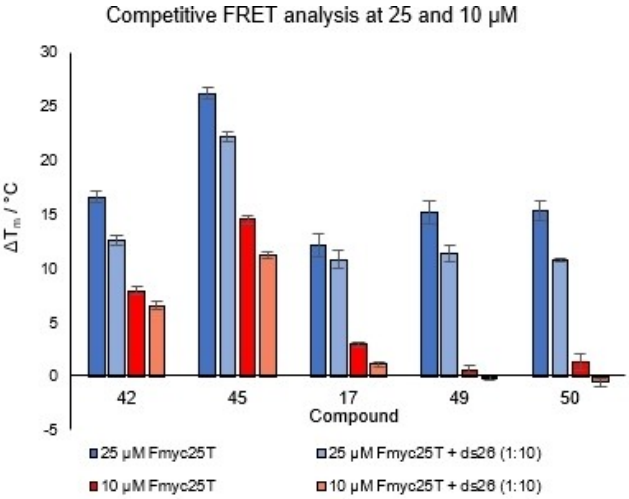

Figure 5. Competitive FRET analysis at 25 μM and 10 μM using F-myc25T and ds26 in the 1:10 ratio. The assay was performed only for selected compounds that exhibited significant FRET activity at 50 μM.

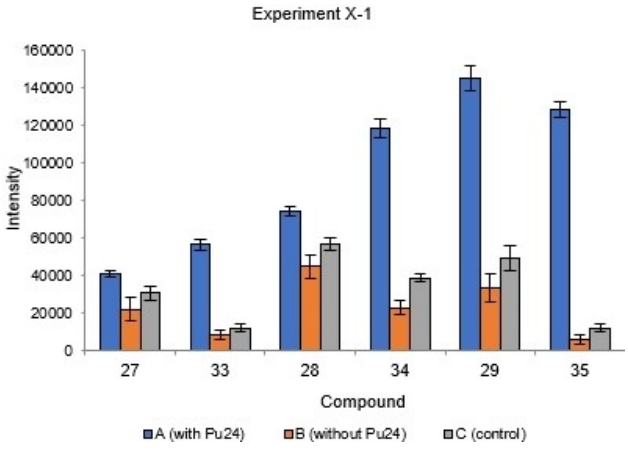

Figure 6. Average intensity of click products **27**–**29** and **33**–**35** during in situ click experiment X-1.

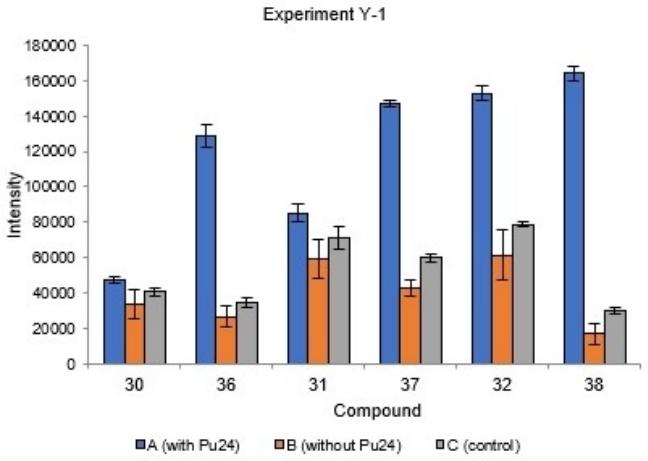

Figure 7. Average intensity of click products **30**–**32** and **36**–**38** during in situ click experiment Y-1.

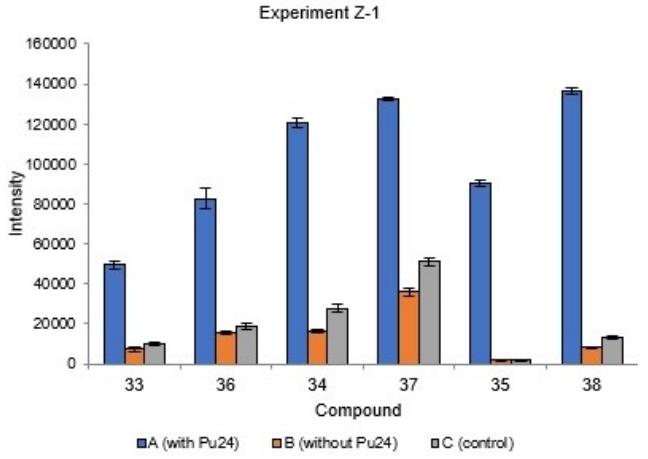

Figure 8. Average intensity of click products **33**–**38** during in situ click experiment Z-1.

assays in the presence of the 10-fold excess of ds26, all compounds retained their *c-MYC* stabilization ability. However, a significant ΔT_m decrease was observed at lower ligand concentration, especially for click products **49** and **50** that showed almost zero activity at 10 μM. Moreover, activity of compounds **17** and **42** at 10 μM was below 10 °C. Therefore, competitive FRET measurements at lower concentrations were not performed as no compound activity would be expected.

Additionally, control PEA experiments were performed with selected compounds to exclude a different inhibition mechanism of the polymerase chain reaction, e.g. by forming a non-canonical PEA bulge. In regard of the control assay, we used a G4-non-forming oligonucleotide template 'Pu27 all-mut' along with Pu27 on the same gel. In this control assay, we tested the parent compound **7** (100 μM) and its bis-amino analogue **17** (100 μM), the well-established *c-MYC* ligand TMPyP4 (1 μM),[5] 1-methyl-1*H*-indol-5-amine (5AMI, 500 μM) reported as a *c-MYC* binder by Nasiri et al,[42] and a KCl solution (100 μM) to observe the effect of G4 stabilization by the K^+ ion. The results (ESI, Section 3.4, Figure S3.10) clearly showed formation of a stop product in the presence of the Pu27 template strand for all compound-containing samples (**7**, **17**, TMPyP4, and 5-AMI) at given concentrations. Moreover, the 100 μM KCl solution produced the stop band as well, as the K^+ ions efficiently stabilized the G4 s formed within the Pu27 sequence. In contrast, no stop band was observed in the presence of the Pu27 all-mut template for any of the samples including the standard TMPyP4, 5AMI, and the KCl solution. Therefore, we can confirm that in PEA, the mechanism of stopping the chain reaction is due to G4 formation induced by the compounds evaluated in this study. Accordingly, the *c-MYC* stabilization potential of the compounds tested corresponds with density of their stop band.

Taken together, both the FRET and PEA assays showed that all compounds of the bis-amino series, especially the compounds **17**, **42**, **45**, **49**, and **45**, are substantially stronger *c-MYC* ligands than compounds of the mono-amino series. The requirement for the free amino group in *para*-position of the aniline moiety was confirmed as the fragments containing amino groups from both series exhibited better *c-MYC* stabilization efficiency in FRET and PEA than their respective nitro- or *o*-nitroaniline- analogues. Furthermore, partial restoration of FRET and PEA activity was observed for mono-amino click products **33**–**38**, which originated from azides **54** and **55** containing a tertiary amino moiety. Moreover, FRET activity of these mono-amino click products **33**–**38** as well as of the bis-amino alkynes **43**–**45** positively correlated with the number of methylene units in the alkynyl linker. Finally, FRET and PEA control experiments performed with G4 non-forming templates confirmed validity and relevance of our measurements.

2.4. KTGS Using In Situ Click Experiments

To evaluate the co-catalytic activity of G4 on formation of the respective click products, a series of in situ click experiments employing the 1,3-dipolar azide-alkyne cycloaddition was carried out. However, KTGS was performed only for the mono-amino series, because the bis-amino alkynes **43**–**45** suffered from poor stability as reported above regarding their synthesis and isolation. It was assumed that performing a direct click reaction of the bis-amino alkynes **43**–**45** with azides **52**–**55** in aqueous solution, in the presence of air, and under prolonged (2-hour) incubation at RT would lead to a quick oxidation of the bis-amino moiety. Additionally, we decided to carry out all in situ click experiments with a catalytic amount of Cu^I species, as our preliminary experiments serving for layout optimization did not show any product formation in the absence of copper catalysis (data not shown). The same finding regarding the lack of product formation in the absence of the Cu^I species was also reported earlier in the study targeting H-Telo.[38]

For the mono-amino series, three sets of copper catalyzed in situ click experiments were set up.[38] Each experiment combined three homologous alkynes **24**–**26** with two different azides to form the 1,4-click products (the combination reactions of three alkynes with the corresponding azides are denoted

here as X, Y and Z). For the products of X, Y, and Z reactions, three different in situ click experiments were performed simultaneously: with Pu24 (A), without Pu24 (B), and a control reaction (C), wherein Pu24 was added just before quenching the reaction with TFA. All experiments were performed in triplicates.

Experiment X consisted of in situ click reactions of alkynes **24**–**26** with azides **52** and **54** resulting in the click products **27**–**29** and **33**–**35**, respectively. Experiment Y combined alkynes **24**–**26** with azides **53** and **55** resulting in click products **30**–**32** and **36**–**38**, respectively. Based on previously performed PEA measurements that identified the click products of azides **54** and **55** more active than click products derived from azides **52** and **53**, we performed an additional in situ click reactions (experiment Z) combining alkynes **24**–**26** with azides **54** and **55** to obtain click products **33**–**38**. The average yields of the in situ click experiments A–C for all 6 products of reactions X–Z are shown in Figure 6 and 5 and in ESI, Section 7, Table S7.1, S7.3, S7.5 and Chart S7.1, S7.3, S7.5. The LC residues (alkyne precursors) are shown in ESI, Section 7, Table S7.2, S7.4, S7.6 and Chart S7.2, S7.4, S7.6.

In a standard in situ click experiment, detecting a click product in a templated reaction directly suggests the templating effect. However, the amounts of the triazole formed in complex reaction mixtures are usually small and difficult to detect and quantify. Therefore, all in situ click experiments contained catalytic copper[38] to increase triazole adduct formation and to facilitate subsequent analysis. Furthermore, the co-catalytic effect of Pu24 G4 is expressed as an A/B ratio of area integral of specific m/z in experiment A (with Pu24) and B (without Pu24). Experiment C and the related A/C ratio were introduced to assess the Pu24 effect on the LC/MS analysis. All compounds **27**–**38** were prepared with increased yields in the presence of Pu24, thus suggesting a possible co-catalytic activity for G4 during the formation of the click products (Table 2, A/B and A/C ratios).

Our data revealed that the presence of three methylene units at the alkynyl chain attached to the N^4 position of the piperazine moiety increased the stability and yield of the reaction products **29**, **32**, **35**, and **38**, with no significant differences in compounds with one and two methylene units (Table 3). Moreover, the A/B and A/C ratios of in situ click products derived from azides **54** and **55** were higher than those of click products derived from azides **52** and **53**. In this regard, click products **33**–**35** derived from azide **54** had the highest A/B and A/C ratios. Compound **35** had the highest yield of the in situ click experiments, followed by **38**, both of which were derived from compound **26** with the longest alkynyl linker (3 methylene units). These results were in agreement with the previously performed SAR study (Table 2) except for compound **38**, which showed higher activity in PEA than **35**. Interestingly, the control reaction C showed small but significant increases in reaction yields when compared with B, suggesting that adding Pu24 oligonucleotide just before quenching leads to rapid click product formation. Therefore, the A/B ratio should be considered the corresponding relative formation yield of a compound.

Furthermore, control in situ click experiments were performed to confirm that the co-catalytic activity of the Pu24 oligonucleotide on ligand assembly is due to the G4 secondary structure formed.

The control in situ click experiments were carried out with a 26-mer 'Q sequence' (ds26) that forms a double-stranded hairpin,[52] and in the same manner as the standard in situ click experiments using the G4-forming Pu24 oligonucleotide. The results (ESI, Section 7, Table S7.7, S7.9, S7.11 and Chart S7.7, S7.9, S7.11 for click products; Table S7.8, S7.10, S7.12 and Chart S7.8, S7.10, S7.12 for alkyne precursors) showed no remarkable product formation increase in experiments A with ds26 over experiments B without ds26 and the control experiment C, because the A/B and A/C ratios were in most cases close to 1.0 (ESI, Section 7, Table S7.13). A substantial A/B and A/C ratio decrease for some compounds – especially for click products **27**, **28**, and **30** derived from azides **52** and **53** with a primary amino moiety-suggests their binding to the double-stranded ds26 sequence. Nevertheless, based on the results obtained, we can assume that the increase of click product formation in presence of Pu24 is the outcome of the *c-MYC* G4 co-catalytic activity.

Overall, KTGS performed for the mono-amino series in the presence of a copper catalyst showed the same SAR trends regarding *c-MYC* affinity as FRET and PEA biology assays. The formation yield in the presence of Pu24 was substantially higher for click products containing three methylene units at the piperazine-triazole linker than for compounds with one and two methylene units. It is apparent that increased flexibility of the aliphatic linker attached to the central scaffold facilitates suitable orientation of key structural motifs and thus efficient interaction of the ligand with *c-MYC*. Moreover, the yield of click product formation derived from azides **54** and **55** containing a tertiary amino moiety was higher than for click products derived from azides **52** and **53** bearing a primary amino moiety.

Our results of control in situ click experiment with G4 non-forming oligonucleotide showed no substantial increase of click product formation. Therefore, we can suppose that the click product formation yield increase in presence of Pu24 is due to the *c-MYC* G4 co-catalytic activity.

2.5. Structural Basis of Compound Binding

The G4 core of Pu24 is formed by the three guanine tetrads (Figure 4A; ESI, Section 8, Figure S8.1).[4–5] To assess the binding modes of the studied compounds, we followed chemical shift changes in the guanine imino-region of ^{1}H NMR spectra of the Pu24-formed G4 upon ligand addition. In particular, the compounds were sorted based on the perturbation or disappearance of individual assigned imino signals in Pu24 into three distinct classes (Figure 4B). The class I ligands induced 5′ G-tetrad destabilization because the imino signals of G4, G13, G8 and G17 disappeared. The residues from the central (G18, G5, G14) and from the 3′ (G15, G6, G19) G-tetrad were shifted significantly, indicating stacking or intercalation of these compounds. The class II compounds induced perturbations

within the 5′ G-tetrad (G4, G13, G8 and G17) and central G-tetrad (G5, G14), indicating stacking of the ligand on the top. The class III compounds induced only perturbations of two guanine NH signals from the 5′ G-tetrad (G4, G17), suggesting a specific interaction with only a minimal effect on the overall conformation of the Pu24 oligonucleotide. The compounds inducing no significant change in the imino region were classified as non-binders.

The classification is summarized in Figure 9B (schematic changes within NMR spectra are shown in ESI, Sections 8.1–8.4, Figures S8.2–S8.6). The class I binders **42**, **49**, **50**, and **17** (ESI, Section 8.1, Figure S8.2) contained a bis-amino moiety and exhibited high Pu24-stabilizing activity in both PEA and FRET. In addition, **49** and **50** were the most active click products prepared in this study. All the class I binders induced significant shifts in selected peaks and extreme broadening of other peaks, indicating 5′ G-tetrad disruption and possible binding on the top of the central tetrad or a ligand intercalation between the central tetrad and the 3′ tetrad. The class II binders comprised the homology series of bis-amino *N*-alkynylated derivatives **43**–**45** and the *o*-nitroaniline click products **47** and **48** (ESI, Section 8.2, Figure S8.3). These ligands were selectively bound only to the 5′ G-tetrad, and this mode of interaction did not disrupt the G4 structure. The compounds in class III carried a nitro group: **46** and **51** were *o*-nitroaniline derivatives, and **40** was a click product with a nitro group on the aromatic ring and served as a negative control for compound **38** in SAR (ESI, Section 8.3, Figure S8.4). This interaction mode should be the weakest because only two guanine NH signals from the 5′ G-tetrad were affected. Moreover, chemical shift changes were only moderate compared with class I and II compounds. Correspondingly, the activity of **40**, **46** and **51** was similar to that of the negative control in PEA and lower than that of **7** in FRET.

No significant effects were observed in the imino regions of NMR spectra of all mono-amino click products **27**–**38**, their *N*-alkynylated clickable precursors **24**–**26**, non-alkylated *o*-nitroaniline derivative **41**, compound **12** as a nitro-analog of **7** and, surprisingly, compound **7** itself (ESI, Section 8.4, Figure S8.5 and S8.6). For compounds **12**, **24**–**26**, and **41** and for most mono-amino click products, this result is consistent with FRET (zero or only partially restored activity compared to **7**) and PEA (activity similar to negative control) assays, which suggest low binding affinity to *c-MYC* G4. However, this category also includes the template molecule **7** and several mono-amino click products, **34**, **35**, **37**, and **38**, which exhibited some stabilizing activity both in FRET or PEA, and their formation was promoted in the presence of Pu24 during in situ click experiments. Hence, these compounds likely have an alternative binding mechanism, which does not perturb imino groups in the core G4 tetrads. Notably, mono-amino click products **27**–**32** that exhibited small negative ΔT_m values in FRET, were also classified as non-binders by ^{1}H NMR as they did not induce any G4 signal perturbation.

In summary, we evaluated compounds of our fragment library for their *c-MYC* G4 binding mode using ^{1}H NMR spectroscopy. Based on our results, it is apparent that the bis-

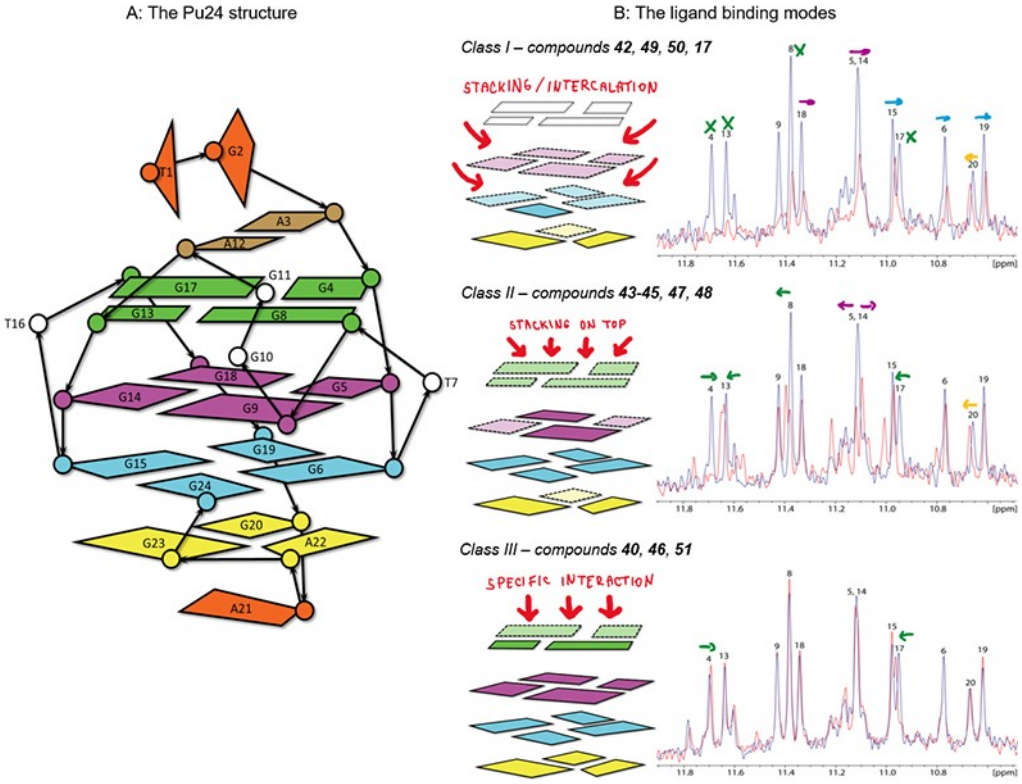

Figure 9. (A) Schematic representation of the Pu24 oligonucleotide. Individual G-tetrads are color-coded.[47] (B) Three distinctive classes of binding ligands were identified by changes in the peaks of individual guanine NH groups within the amidic region of ^{1}H NMR.

amino compounds **17**, **42**, **49**, and **50** that belonged to the most active ligands according to FRET and PEA biology assay also exhibited the strongest *c-MYC* binding mode (class I binders). Additionally, most of the remaining compounds of the bis-amino series belonged either to the binder class II or III, both of which represent a weaker binding mode. On the other hand, all compounds of the mono-amino series, including the parent compound **7**, were determined as non-binders. These findings are in accordance with FRET and PEA results that revealed mono-amino compounds as less active than compounds of the bis-amino series.

3. Conclusions

Stabilization of G-quadruplexes formed in the *c-MYC* promoter region may be a viable strategy for anticancer therapy. We used the 4-(4-methylpiperazin-1-yl)aniline molecule, identified in a previously published study[42] as a c-MYC ligand, as a template for the SAR-guided design of a small focused fragment library suitable for click chemistry. The biochemical assays revealed that the presence of a free amino substituent at the aromatic ring was essential for stabilizing potency of this type of molecules and that an additional amino group at position 2 further increased their activity. Moreover, the piperazine ring was amenable to N^4-alkynylation, which allowed subsequent click reactions, with an optimal length of three methylene units. We subjected the scaffolds to 'conventional' and in situ click reactions in the presence of Pu24. For the mono-amino click products, the G4-stabilizing activity and their in situ formation yield positively correlated with the increase in the number of methylene units in the alkynyl chain. Similarly, in the bis-amino series of *N*-alkynyl derivatives, we observed no change in activity in compounds with one and two methylene units, but we detected significant increases in activity in compounds with three methylene units. Using ^{1}H NMR spectroscopy, we probed the mode of interaction for the studied compounds. Interestingly, the most potent bis-amino compounds, including the *N*-alkynyl homologs and their click products, were destabilizing the 5′ guanine tetrad and most likely stacking on the top of the central tetrad. Our study suggests that the bis-amino derivatives of the 4-(piperazin-1-yl)aniline template, including the click products, appear to be potent *c-MYC* G4 stabilizers in FRET, PEA, and NMR at low micromolar concentrations and may be amenable to further therapeutic development.

Experimental Section

Oligonucleotides

The HPLC-purified Pu24 oligo-deoxyribonucleotide mimicking *c-MYC* G4 as well as the HPLC-purified ds26 oligo-deoxyribonucleotide forming a double-stranded hairpin were purchased in lyophilized form from Generi Biotech (www.generi-biotech.com):

Pu24: 5′-TGA GGG TGG GGA GGG TGG GGA AGG-3′

Ds26: 5′-TAT AGC TAT ATT TTT TTA TAG CTA TA-3′

Each lyophilizate was dissolved in 20 mM KH_2PO_4, 70 mM KCl, NaN_3 (0.02%), pH 7.0 to the final concentration of 15 μM. Subsequently, the solution was annealed at 95 °C for 15 minutes and allowed to gradually cool down to room temperature (RT), adopting the typical 'propeller' shaped conformation.

FRET

The dual-labelled oligonucleotides Fc-myc25T and FdsT (5′-FAM and 3′-TAMRA) were purchased from Sigma-Aldrich®. Regarding Fc-myc25T, the shorter sequence of the NHEIII1 region (Pu27 or *c-MYC* G4) was used. This sequence contains only five G-tracts, enabling folding in 1–4 and 2–5 *c-MYC* G4 conformers. The last GG was removed to increase FRET efficiency. The sequence of the Fc-myc25T oligonucleotide is:

Fc-myc25T: 5′-FAM-TGGGGAGGGTGGGGAGGGTGGGGAA-TAMRA-3′

On the contrary, the FdsT used for control measurements contained a 26-mer Q-sequence (ds26) forming a double-stranded hairpin:

FdsT: 5′-FAM-TATAGCTATATTTTTTTATAGCTATA-TAMRA-3′

All FRET melting experiments were performed in 10 mM Cacodylate buffer (pH = 7.2) containing 95 mM LiCl and 5 mM KCl. Oligonucleotides were heat-denatured at 95 °C for 10 minutes and cooled by approximately 1 °C per minute to RT. A 384-well plate was used, with each well containing the dual-labelled oligonucleotide at a final concentration of 0.2 μM in 20 μl. In competitive FRET experiments with 0.2 μM of F-myc25T, ten-fold excess of non-labelled ds26 oligonucleotide was added to the mixture to reach the final concentration of 2.0 μM. All compounds dissolved in DMSO to a concentration of 10 mM were loaded into the wells using an ECHO® 550 acoustic liquid handler with final concentrations of 100 μM with 1% DMSO. Melting curves were measured on a LightCycler® 480 Instrument II by monitoring FAM fluorescence (Syber green I channel, with excitation wavelength at 465 nm and emission at 510 nm). Melting points were calculated in GraphPad Prizm 5 using the asymmetric five parameter model. The ability of a particular fragment to stabilize the secondary structure of the Pu25 (Fc-myc25T) or ds26 (FdsT) oligonucleotide was expressed as a difference between the melting points of the sample and of a control. Each test was performed in duplicates and repeated in three independent experiments (n = 3).

DNA Polymerase Extension Assay (PEA)

In PEA, the movement of DNA polymerase on the template produces a stop band if the G4 blocks are folded.[53] Both the primer and the template were purchased from Sigma-Aldrich® (www.sigmaaldrich.com). The primer was labelled on the 5 – end with ^{32}P using T4 polynucleotide kinase (TaKaRa ref: 2021 A) according to the manufacturer's instructions. P-30 colons were used to remove unbound radioactivity. The labelled primer and the template were mixed in water in a 1:1.25 ratio, heat-denatured at 95 °C for 10 minutes and cooled approximately 1 °C per minute to RT. The template concentration in the primer/template mixture was 12.5 μM. The polymerase stop reaction was performed using a GoTaq® G2 DNA polymerase kit (PROMEGA ref: M784A); the reaction was run in 1X Colorless GoTaq® Reaction Buffer. The final reaction volume was 20 μl and contained 0.1 μM template (primer/template mixture), 200 μM dNTP, and either compounds in DMSO solution or DMSO as a control. The reaction started after 30-minute incubation at 52 °C (optimized temperature) by adding 2 μL of DNA polymerase (1 U/μL) to reach 0.1 U per well and further incubated at 52 °C for 30 minutes. At the end, the reaction was stopped by adding 5x loading solution (80% formamide, 10% glycerol, 20 mM EDTA pH 8,

0,025% xylene cyanol and 0,025% bromophenol blue), heat-denatured for 5 minutes at 95 °C, subsequently cooled on ice and kept at −20 °C until separation on a 15% AA denaturating gel containing 40% of urea at 55 °C, vacuum dried and visualized using phosphoimaging cassettes and scanned on the Typhoon™ FLA 5500 at 100 μM resolution. Band densities were evaluated by Image Quant software and data were normalized using the following formula:

$$Ligand\ rel.\ stop\ product = \frac{Ligand\ stop\ product / Ligand\ (stop\ product + full - length\ product)}{Control\ stop\ product / Control\ (stop\ product + full - length\ product)}$$

The data were determined as a quotient of stop band density of the respective compound divided by the stop band density of the parent compound **7**, which was present on each gel. All compounds were screened at 100 μM concentration with 5% of DMSO.

Template Pu27: 5′-CTGCGATCCGTCAGTCCAACATGCTATACT-

-GGGGAGGGTGGGGAGGGTGGGGAAGG-

TTAGCGGCACGCAATTGCTAGCGTGAGTCG-3′

Reverse primer: 5′-CGACTCACGCTAGCAATTGCGTG-3′

For control PEA measurement, the template strand containing the Pu27 'all-mut' sequence incapable of G4 formation was used:

Pu27 'all-mut': 5′-CTGCGATCCGTCAGTCCAACATGCTATACT-

-GAAGAGAGTGAAGAGAGTGAAGAAGG-

TTAGCGGCACGCAATTGCTAGCGTGAGTCG-3′

Chemistry

The mono-amino series (Figure 3A) was synthesized via an *N*-alkylation reaction of the piperazine moiety at the 4-(piperazin-1-yl) aniline with the respective alkynyl halides under basic conditions,[54] thereby preparing a homologous series of three 4-(piperazin-1-yl) aniline-derived alkynes with different alkynyl chain lengths, **24**,[45] **25**, and **26** (ESI, Section 4, Scheme S-1). Compounds from the bis-amino series (Figure 3B) were synthesized as follows: firstly, compound **41** was prepared by nucleophilic aromatic substitution of 5-chloro-2-nitroaniline with piperazine under basic conditions, then reduced by catalytic hydrogenation on Pd/C forming the compound **42** (ESI, Section 4, Scheme S-2).[46] Finally, **42** was *N*-alkylated under basic conditions[54] with the respective alkynyl halide to obtain compounds **43**–**45** (ESI, Section 4, Scheme S-2). The alkyne derivatives of both families formed 1,4-disubstituted triazole compounds by CuAAC.

The alkynyl compounds from the mono-amino series, **24**–**26** (Figure 3A), were directly mixed with 3-azido-*N*,*N*-dimethylpropan-1-amine in the presence of catalytic amounts of Cu^{I} upon triazole formation.[38] The CuAAC reaction products **33**–**35** showed sufficient yields (ESI, Section 4, Scheme S-3). Similarly, CuAAC reactions were performed with 1-(2-azidoethyl)pyrrolidine[38] to form compounds **36**–**38**, with 2-azidoethan-1-amine to form compounds **27**–**29**, and with 3-azidopropan-1-amine to form compounds **30**–**32**. All click products were isolated in good yields (ESI, Section 4, Scheme S–3).

A direct CuAAC reaction of the bis-amino derivatives (Figure 3B, **43**–**45**) was not performed due to the low stability of the *o*-phenylendiamine moiety. Instead, the nitro compound **41** was alkylated under basic conditions in the presence of 5-iodopent-1-yne[54] to form **46** (ESI, Section 4, Scheme S-5). Then, subsequent CuAAC reactions of **46** with 3-azido-*N*,*N*-dimethylpropan-1-amine or 1-(2-azidoethyl)pyrrolidine were performed to form compounds **47** and **48** (ESI, Section 4, Scheme S-5). Both **47** and **48** were subsequently reduced by hydrogenation on Pd/C[46] to their bis-amino counterparts, **49** and **50**. To avoid decomposition of the bis-amino compounds, the respective hydrochloride salts were formed immediately after quenching the hydrogenation reaction by adding the HCl-ethanol solution.

Furthermore, 1-(4-nitrophenyl)piperazine was alkylated with 5-iodopent-1-yne under basic conditions[54] to form compound **39**, which was then mixed with 1-(2-azidoethyl)pyrrolidine in the presence of catalytic amounts of Cu^{I} to afford the compound **40** (ESI, Section 4, Scheme S-4). Lastly, compounds **41** and **17** were prepared as described for **41** and **42**: in a nucleophilic aromatic substitution, 5-chloro-2-nitroaniline was mixed with 1-methylpiperazine to form **51**,[55] and compound **17** was prepared from **51** by reduction of its nitro group by catalytic hydrogenation on Pd/C.[55] The decomposition of the bis-amino compound **17** was avoided by immediate formation of hydrochloride salt (ESI, Section 4, Scheme S-6).

In Situ Click Experiments

The reaction mixture for each in situ click experiment contained three alkynes (1.0 mM each), two azides (1.5 mM each), Tris-HCl buffer (15 mM, pH 7.4), KCl (100 mM), $CuSO_4$ (1.5 mM) and sodium ascorbate (3.0 mM), with (experiment A) or without (experiments B and C) the oligonucleotide Pu24 or ds26 (both 0.1 mM in Tris-HCl/KCl buffer). In the control experiment (C), the respective oligonucleotide was added to the reaction mixture only 1 minute before quenching the reaction (for more detailed experimental setup, see ESI, Section 6, Table S6.1-S6.3). After 2 hours of shaking at 300 rpm, 22 °C, trifluoroacetic acid (TFA, 40% in H_2O) was added to quench the reaction by denaturing the DNA. The composition of each reaction mixture was analyzed by LC–MS. The ratio of the integral amount measured by LC–MS of each click product was calculated between experiments A and B (A/B ratio) and between experiments A and C (A/C ratio).

LC–MS Evaluation of in Situ Click Experiments

Samples were injected onto a Luna Omega Polar C18 column 150x1.0 mm (Phenomenex) and separated by gradient of acetonitrile in water (both mobile phases modified by 0.1% formic acid). The separation was performed by an LC system (I-class, Waters) coupled to Mass Spectrometer (Synapt G2, Waters) to acquire m/z by positive electrospray ionization in the range of 100–1500 m/z. The extracted ion chromatogram of the monitored peaks was integrated by Quantlynx application of MassLynx 4.1 (Waters).

Hit Validation by ^{1}H NMR Spectroscopy

For the purpose of hit validation by ^{1}H NMR, all tested compounds were dissolved in DMSO-d_6 to the final concentration of 20 mM. The samples were formulated on one-to-one basis to avoid false-positive hits caused by aggregation of ligands or misinterpretation of complex spectra of mixtures. The stock solution of the target (Pu24) was prepared to match the final concentration of 5 μM, adding 10% D_2O for field locking, in an NMR buffer (pH = 7.0) containing 20 mM KH_2PO_4, 70 mM KCl, and 0.02% NaN_3. Individual ligand solutions were added to a G4 stock solution to match the final 100x excess of ligand (500 μM) over target. Each tested sample was formulated as follows: 14 μL of the DMSO-d_6 solution

containing the respective ligand in 20 mM concentration was added to 536 μL of 5 μM G4 stock solution containing 10% D_2O to obtain final sample volume of 550 μM. This formulation introduced 2.5% of DMSO-d_6 from the compound's stock solutions. The peak of the residual DMSO-d_6 ($\delta = 2.50$ ppm) was used as an internal reference standard. Therefore, there was no need to add additional internal reference standard which could possibly interfere in the STD ^{1}H NMR experiment.

All samples were spun down in Eppendorf Minispin Centrifuge at 12.100 x g for 2 minutes to separate possible aggregates and to remove air bubbles. The samples were transferred into NMR tubes and stored at 4 °C. The ^{1}H NMR experiment was performed on a Bruker Avance III™ HD 600 MHz spectrometer equipped with a Cryoprobe and a sample changer (for a detailed spectrometer setup, see ESI, Section 8). The ^{1}H NMR spectra were acquired using 350/550μL samples of 5 μM Pu24 dissolved in NMR buffer at 293 K and the standard 'stddiffesgp'[56–57] pulse sequence with excitation sculpting and pulse-field gradients for water suppression. The frequency of non-selective irradiation pulse was set to saturate the well-separated signal of DNA (6824 Hz, amidic region), using a 50 ms shaped Eburp2.1000 pulse at a power of 40 dB. The irradiated signals had to be sufficiently separated from the ligand's signals to prevent their direct irradiation, which would generate false positive hits. The spectra were acquired at a free induction decay (FID) resolution of ~1 Hz. The typical experimental time of each sample was 30 minutes, thus allowing measurements of the whole library within one day.

Acknowledgements

This work was supported by grants from GACR (17-04393S), the Ministry of Education of the Czech Republic (LO1304, LM2015070 and LK11205), the European Regional Development Fund; OP RDE; Project: "Chemical biology for drugging undruggable targets (ChemBioDrug)" (No. CZ.02.1.01/0.0/0.0/16_019/0000729). and the Czech Academy of Sciences (RVO61388963). We thank Katarina Psenakova and Carlos Melo for valuable comments and proof-reading of the manuscript.

Conflict of Interest

The authors declare no conflict of interest.

Keywords: anticancer therapy · click chemistry · G-quadruplex · NMR · secondary structures

[1] S. Neidle, *J. Med. Chem.* **2016**, *59*, 5987–6001.
[2] J. B. Chaires, D. Graves, *Quadruplex nucleic acids*, SPRINGER, **2013**.
[3] N. Campbell, G. W. Collie, S. Neidle, *Curr. Protoc. Nucleic Acid Chem.* **2012**, *50*, 17.6.11-17.6.22.
[4] S. Balasubramanian, L. H. Hurley, S. Neidle, *Nat. Rev. Drug Discovery* **2011**, *10*, 261–275.
[5] A. Siddiqui-Jain, C. L. Grand, D. J. Bearss, L. H. Hurley, *PNAS* **2002**, *99*, 11593–11598.
[6] W. P. Tansey, *New J. Sci.* **2014**, *2014*, 27.
[7] N. Meyer, L. Z. Penn, *Nat. Rev. Cancer* **2008**, *8*, 976–990.
[8] C. Y. Lin, J. Lovén, P. B. Rahl, R. M. Paranal, C. B. Burge, J. E. Bradner, T. I. Lee, R. A. Young, *Cell* **2012**, *151*, 56–67.
[9] T. A. Brooks, L. H. Hurley, *Nat. Rev. Cancer* **2009**, *9*, 849–861.
[10] D. Yang, L. H. Hurley, *Nucleos. Nucleot. Nucl.* **2006**, *25*, 951–968.
[11] M. L. Bochman, K. Paeschke, V. A. Zakian, *Nat. Rev. Genet.* **2012**, *13*, 770–780.
[12] Y. Qin, L. H. Hurley, *Biochimie* **2008**, *90*, 1149–1171.
[13] A. T. Phan, V. Kuryavyi, H. Y. Gaw, D. J. Patel, *Nat. Chem. Biol.* **2005**, *1*, 167–173.
[14] J. Seenisamy, E. M. Rezler, T. J. Powell, D. Tye, V. Gokhale, C. S. Joshi, A. Siddiqui-Jain, L. H. Hurley, *J. Am. Chem. Soc.* **2004**, *126*, 8702–8709.
[15] A. Ambrus, D. Chen, J. Dai, R. A. Jones, D. Yang, *Biochemistry* **2005**, *44*, 2048–2058.
[16] D. Monchaud, M.-P. Telaude-Fichou, *Org. Biomol. Chem.* **2008**, *6*, 627–636.
[17] B.-J. Chen, Y.-L. Wu, Y. Tanaka, W. Zhang, *Int. J. Biol. Sci.* **2014**, *10*, 1084–1096.
[18] S. Maiti, N. K. Chaudhury, S. Chowdhury, *Biochem. Biophys. Res. Commun.* **2003**, *310*, 505–512.
[19] T.-M. Ou, Y.-J. Lu, C. Zhang, Z.-S. Huang, X.-D. Wang, J.-H. Tan, Y. Chen, D.-L. Ma, K.-Y. Wong, J. C.-O. Tang, A. S.-C. Chan, L.-Q. Gu, *J. Med. Chem.* **2007**, *50*, 1465–1474.
[20] Y.-J. Lu, T.-M. Ou, J.-H. Tan, J.-Q. Hou, W.-Y. Shao, D. Peng, N. Sun, X.-D. Wang, W.-B. Wu, X.-Z. Bu, Z.-S. Huang, D.-L. Ma, K.-Y. Wong, L. Q. Gu, *J. Med. Chem.* **2008**, *51*, 6381–6392.
[21] Y. Ma, T.-M. Ou, J.-Q. Hou, Y.-J. Lu, J.-H. Tan, L.-Q. Gu, Z.-S. Huang, *Bioorg. Med. Chem.* **2008**, *16*, 7582–7591.
[22] B. Dumat, G. Bordeau, E. Faurel-Paul, F. Mahuteau-Betzer, N. Saettel, M. Bombled, G. Metgé, F. Charra, C. Fiorini-Debuisschert, M.-P. Teulade-Fichou, *Biochimie* **2011**, *93*, 1209–1218.
[23] A. Rangan, O. Y. Fedoroff, L. H. Hurley, *J. Biol. Chem.* **2001**, *276*, 4640–4646.
[24] D.-L. Ma, V. P.-Y. Ma, K.-H. Leung, H.-J. Zhong, H.-Z. He, D. S.-H. Chan, C.-H. Leung, *Structure-Based Approaches Targeting Oncogene promoter G-Quadruplexes*, InTech, **2013**.
[25] W. Duan, A. Rangan, H. Vankayalapati, M.-Y. Kim, Q. Zeng, D. Sun, H. Han, O. Y. Fedoroff, D. Nishioka, S. Y. Rha, E. Izbicka, D. D. Von Hoff, L. H. Hurley, *Mol. Cancer Ther.* **2001**, *1*, 103–120.
[26] H. Mo, M. Vita, M. Crespin, M. Arsenian Henriksson, *Cell Cycle* **2006**, *5*, 2191–2194.
[27] Y. Jiang, A.-C. Chen, G.-T. Kuang, S.-K. Wang, T.-M. Ou, J.-H. Tan, D. Li, Z.-S. Huang, *Eur. J. Med. Chem.* **2016**, *122*, 264–279.
[28] D. Dutta, M. Debnath, D. Müller, R. Paul, T. Das, I. Bessi, H. Schwalbe, J. Dash, *Nucleic Acids Res.* **2018**, *46*, 5355–5365.
[29] S. Pelliccia, J. Amato, D. Capasso, S. Di Gaetano, A. Massarotti, M. Piccolo, C. Irace, G. C. Tron, B. Pagano, A. Randazzo, E. Novellino, M. Giustiniano, *J. Med. Chem.* **2020**, *63*, 2035–2050.
[30] A. Chauhan, R. Paul, M. Debnath, I. Bessi, S. Mandal, H. Schwalbe, J. Dash, *J. Med. Chem.* **2016**, *59*, 7275–7281.
[31] W. G. Lewis, L. G. Green, F. Grynszpan, Z. Radić, P. R. Carlier, P. Taylor, M. G. Finn, K. B. Sharpless, *Angew. Chem. Int. Ed. Engl.* **2002**, *41*, 1053–1057.
[32] M. Whiting, J. Muldoon, Y.-C. Lin, S. M. Silverman, W. Lindstrom, A. J. Olson, H. C. Kolb, M. G. Finn, K. B. Sharpless, J. H. Elder, V. V. Fokin, *Angew. Chem. Int. Ed.* **2006**, *45*, 1435–1439; *Angew. Chem.* **2006**, *118*, 1463–1467.
[33] X. Hu, R. Manetsch, *Chem. Soc. Rev.* **2010**, *39*, 1316–1324.
[34] S. K. Mamidyala, M. G. Finn, *Chem. Soc. Rev.* **2010**, *39*, 1252–1261.
[35] N. P. Grimster, B. Stump, J. R. Fotsing, T. Weide, T. T. Talley, J. G. Yamauchi, Á. Nemecz, C. Kim, K.-Y. Ho, K. B. Sharpless, P. Taylor, V. V. Fokin, *J. Am. Chem. Soc.* **2012**, *134*, 6732–6740.
[36] I. Glassford, C. N. Teijaro, S. S. Daher, A. Weil, M. C. Small, S. K. Redhu, D. J. Colussi, M. A. Jacobson, W. E. Childers, B. Buttaro, A. W. Nicholson, A. D. MacKerell, B. S. Cooperman, R. B. Andrade, *J. Am. Chem. Soc.* **2016**, *138*, 3136–3144.
[37] D. Bosc, J. Jakhlal, B. Deprez, R. Deprez-Poulain, *Future Med. Chem.* **2016**, *8*, 381–404.
[38] M. Di Antonio, G. Biffi, A. Mariani, E.-A. Raiber, R. Rodriguez, S. Balasubramanian, *Angew. Chem. Int. Ed.* **2012**, *51*, 11073–11078; *Angew. Chem.* **2012**, *124*, 11235–11240.
[39] M.-H. Hu, X. Chen, S.-B. Chen, T.-M. Ou, M. Yao, L.-Q. Gu, Z.-S. Huang, J.-H. Tan, *Sci. Rep.* **2015**, *5*, 17202.
[40] D. Panda, P. Saha, T. Das, J. Dash, *Nat. Commun.* **2017**, *8*, 16103.
[41] P. Thirumurugan, D. Matosiuk, K. Jozwiak, *Chem. Rev.* **2013**, *113*, 4905–4979.
[42] H. R. Nasiri, N. M. Bell, K. I. E. McLuckie, J. Husby, C. Abell, S. Neidle, S. Balasubramanian, *Chem. Commun.* **2014**, *50*, 1704–1707.
[43] S. A. Latt, G. Stetten, *J. Histochem. Cytochem.* **1976**, *24*, 24–33.

[44] P. E. Pjura, K. Grzeskowiak, R. E. Dickerson, *J. Mol. Biol.* **1987**, *197*, 257–271.
[45] M. D. P. Risseeuw, D. J. H. De Clercq, S. Lievens, U. Hillaert, D. Sinnaeve, F. Van den Broeck, J. C. Martins, J. Tavernier, S. Van Calenbergh, *ChemMedChem* **2013**, *8*, 521–526.
[46] T. de la Fuente, M. Martín-Fontecha, J. Sallander, B. Benhamú, M. Campillo, R. A. Medina, L. P. Pellissier, S. Claeysen, A. Dumuis, L. Pardo, M. L. López-Rodríguez, *J. Med. Chem.* **2010**, *53*, 1357–1369.
[47] S. Balasubramanian, S. Neidle, *Curr. Opin. Chem. Biol.* **2009**, *13*, 345–353.
[48] A. R. Duarte, E. Cadoni, A. S. Ressurreicao, R. Moreira, A. Paulo, *ChemMedChem.* **2018**, *13*, 869–893.
[49] Y. P. Kumar, P. Saha, D. Saha, I. Bessi, H. Schwalbe, S. Chowdhury, J. Dash, *ChemBioChem.* **2016**, *17*, 388–393.
[50] N. Ranjan, D. P. Arya, *Molecules* **2013**, *18*, 14228–14240.
[51] L. Yu, Q. Yang, J. Xiang, H. Sun, L. Wang, Q. Li, A. Guan, Y. Tang, *Analyst* **2015**, *140*, 1637–1646.
[52] A. Anselmet, E. Mayat, S. Wietek, P. G. Layer, B. Payrastre, J. Massoulié, *FEBS Lett.* **2002**, *510*, 175–180.
[53] A. Galeone, *ChemBioChem* **2010**, *11*, 2050–2051.
[54] E. Hryhorenko, B. Sankaran, T. R. DeCory, T. Tubbs, L. Colt, B. M. Remmerie, R. Salter, M. G. Donahue, Y. Gong, US 2014/0057303 A1 (27.02.2014).
[55] S. Ramachandran, S. Hameed, P. A. Srivastava, G. Shanbhag, S. Morayya, N. Rautela, D. Awasthy, S. Kavanagh, S. Bharath, J. Reddy, V. Panduga, K. R. Prabhakar, R. Saralaya, R. Nanduri, A. Raichurkar, S. Menasinakai, V. Achar, M. B. Jimenéz-Díaz, M. Santos Martínez, I. Angulo-Barturen, S. Ferrer, L. M. Sanz, F. J. Gamo, S. Duffy, V. M. Avery, D. Waterson, M. C. S. Lee, O. Coburn-Flynn, D. A. Fidock, P. S. Iyer, S. Narayanan, V. Hosagrahara, V. K. Sambandamurthy, *J. Med. Chem.* **2014**, *57*, 6642–6652.
[56] M. Mayer, B. Meyer, *Angew. Chem. Int. Ed.* **1999**, *38*, 1784–1788; *Angew. Chem.* **1999**, *111*, 1902–1906.
[57] T.-L. Hwang, A. J. Shaka, *J. Magn. Reson. Ser. A* **1995**, *112*, 275–279.

Manuscript received: September 4, 2020
Revised manuscript received: November 2, 2020